

**Figure 2.** Angular dependence of the resonance fields of the  $\Delta M_s = \pm 1$  allowed transitions observed at 77 K for the rotation of the magnetic field in the  $ac$  plane ( $\nu = 9587.0$  MHz). The primed and unprimed characters correspond to the two magnetically nonequivalent sites. The solid points represent the observed values and the solid curves the calculated ones.

was obtained in 91% yield by heating **4**, hydrazine hydrochloride, and anhydrous hydrazine in dimethyl sulfoxide at 100 °C for 2 h and then treated with HgO, Na<sub>2</sub>SO<sub>4</sub>, and a small amount of a saturated ethanol solution of KOH at 20 °C for 3 h. Recrystallization twice from *n*-hexane gave **2** as deep-red crystals, 104–110 °C dec: 400-MHz <sup>1</sup>H NMR (CD<sub>2</sub>Cl<sub>2</sub>)  $\delta$  7.0–7.4;  $\lambda_{\max}$  291 ( $\epsilon$  1.20 × 10<sup>5</sup>) and 518 nm (5.20 × 10<sup>2</sup>); IR (KBr) 3050, 2040, 1590, 1480, 680 cm<sup>-1</sup>.

Figure 1a shows a typical ESR spectrum of **1** observed at 50 K, exhibiting a pattern characteristic of the  $\Delta M_s = \pm 1$  allowed transitions from the undecet spin sublevels. This fine structure has been related to  $M_s$  as  $A_{\pm}(\pm 5 \leftrightarrow \pm 4)$ ,  $B_{\pm}(\pm 4 \leftrightarrow \pm 3)$ ,  $C_{\pm}(\pm 3 \leftrightarrow \pm 2)$ ,  $D_{\pm}(\pm 2 \leftrightarrow \pm 1)$ , and  $E_{\pm}(\pm 1 \leftrightarrow 0)$ . The relative separations of each of the pairs in Figure 1a are  $(A_{-}-A_{+}):(B_{-}-B_{+}):(C_{-}-C_{+}):(D_{-}-D_{+}):(E_{-}-E_{+}) = 9.4:7.2:5.1:3.0:1.0$ , which are close to the ratios of 9:7:5:3:1 expected for the fine structure from  $S = 5$  in the high-field limit.

The resonance fields, the signal intensities, and their angular dependence of the observed spectra were described well by the effective spin Hamiltonian,

$$\mathcal{H} = g\beta\vec{H}\cdot\vec{S} + D[S_z^2 - S(S+1)/3] + E(S_x^2 - S_y^2) \quad (1)$$

with  $S = 5$ ,  $g = 2.003$ ,  $D = -0.0168$  cm<sup>-1</sup>, and  $E = +0.0036$  cm<sup>-1</sup>. The observed resonance fields and intensities in Figure 1a agree with those in Figure 1b, which were calculated from eq 1, assuming the negligible Boltzmann factor at 50 K. The angular dependence in Figure 2 confirms the agreement between theory and experiment, proving **1** to be an undecet molecule. To ascertain the undecet ground state, we examined the ESR spectra in the range 5–77 K. Only the spectrum arising from the  $S = 5$  state of **1** was observed as shown in Figure 1, signals due to the  $S = 1, 2, 3$ , and 4 states of **1** being undetected. Furthermore, the total intensity of the undecet lines decreased with increasing temperature, as quantitatively expected for an isolated undecet ground state. Thus, we concluded that the observed undecet state is the electronic ground state of **1**. The negative sign of  $D$  was determined by considering the Boltzmann factor at 5 K.

Hydrocarbon **1** has not only five delocalized unpaired  $\pi$  electrons due to topological symmetry,<sup>2,3</sup> as predicted by the simple MO<sup>9</sup> as well as VB<sup>2,6c,d</sup> theories, but also five localized unpaired electrons in the  $\sigma$  nonbonding orbitals at the five divalent carbon atoms. The spin-density distribution obtained from the UHF calculation using a generalized Hubbard model<sup>4e,6f</sup> gives the following picture. There are five net  $\pi$  spins which are parallel and distributed over the carbon skeleton with changing the sign of spin densities alternately from carbon to carbon, while the other five localized spins are exchange coupled ferromagnetically to the  $\pi$  spins at each divalent carbon atom. Since the  $\pi$  spin densities have the same sign at each of the divalent carbon atoms as de-

termined from topological symmetry, all 10 unpaired spins in **1** are ferromagnetically coupled with each other, leading to the  $S = 5$  ground state. The realization of such an organic high-spin molecule as **1** strongly suggests the possible occurrence of organic superparamagnetism originating from properly designed macro-molecules with extremely large spins.

**Acknowledgment.** The present work was supported by a Grant-in-Aid for General Science Research and for Scientific Research on Priority Areas from the Ministry of Education, Science and Culture.

### Observation of a New Low-Energy Fluorescent <sup>1</sup>( $\pi, \pi^*$ ) Excited State in Strongly Coupled Porphyrin Dimers

Osman Bilsel, Juan Rodriguez, and Dewey Holten\*

Department of Chemistry, Washington University  
St. Louis, Missouri 63130

Gregory S. Girolami,\* Stanley N. Milam, and  
Kenneth S. Suslick\*

School of Chemical Sciences  
University of Illinois at Urbana-Champaign  
Urbana, Illinois 61801

Received December 19, 1989

Elucidating the electronic interaction between porphyrinic macrocycles held in close proximity is crucial to understanding the mechanisms of important biological and chemical processes such as electron transfer in photosynthesis<sup>1</sup> and bimetallic catalysis.<sup>2</sup> This is evident in the photosynthetic reaction center where the interaction between the bacteriochlorophylls of the dimeric primary electron donor (P) gives rise to unusual features such as the long-wavelength band of P in its neutral form or the near-infrared band in its oxidized form.<sup>1</sup> Interestingly, a number of recently synthesized lanthanide and actinide porphyrin sandwich complexes exhibit analogous spectral characteristics, namely, a broad absorption feature immediately to the red of the monomer-like Q bands in the neutral species and a near-infrared band in the oxidized species.<sup>3-7</sup> We report here the first observation of luminescence from bis-porphyrinate complexes, specifically, the neutral complexes of Th<sup>IV</sup>. The location of the fluorescence identifies the absorption immediately to the red of the Q bands as vibronic transitions to a previously unknown <sup>1</sup>( $\pi, \pi^*$ ) state of the dimer. This new ( $\pi, \pi^*$ ) state is the lowest energy excited state in the singlet manifold and apparently arises from substantial porphyrin-porphyrin  $\pi$ -orbital overlap.

(1) (a) Kirmaier, C.; Holten, D. *Photosynth. Res.* **1987**, *13*, 225–260. (b) Budill, D.; Gast, P.; Chang, C. H.; Schifer, M.; Norris, J. R. *Annu. Rev. Phys. Chem.* **1987**, *38*, 561–583. (c) Hanson, L. K. *Photochem. Photobiol.* **1988**, *47*, 903–921. (d) Friesner, R. A.; Won, Y. *Biochim. Biophys. Acta* **1989**, *977*, 99–122.

(2) Durand, R. R., Jr.; Bencosme, C. S.; Collman, J. P.; Anson, F. C. *J. Am. Chem. Soc.* **1983**, *105*, 2710–2718. (b) Collman, J. P.; Anson, F. C.; Barnes, C. E.; Bencosme, C. S.; Geiger, T.; Evitt, E. R.; Kreh, R. P.; Meier, K.; Pettman, R. B. *J. Am. Chem. Soc.* **1983**, *105*, 2694–2699. (c) Ni, C. L.; Abdalmuhdi, I.; Chang, C. K.; Anson, F. C. *J. Phys. Chem.* **1987**, *91*, 1158–1166.

(3) (a) Buchler, J.; Scharbert, B. *J. Am. Chem. Soc.* **1988**, *110*, 4272–4276. (b) Buchler, J.; de Cian, A.; Fischer, J.; Kihn-Botulinski, M.; Weiss, R. *Inorg. Chem.* **1988**, *27*, 339–345. (c) Buchler, J.; de Cian, A.; Fischer, J.; Kihn-Botulinski, M.; Paulus, H.; Weiss, R. *J. Am. Chem. Soc.* **1986**, *108*, 3652–3659. (d) Buchler, J.; Kapellman, H.-G.; Knoff, M.; Lay, K.-L.; Pfeifer, S. Z. *Naturforsch., B: Anorg. Chem., Org. Chem.* **1983**, *38B*, 1339–1345.

(4) Bilsel, O.; Rodriguez, J.; Holten, D. *J. Phys. Chem.*, in press.

(5) Girolami, G. S.; Milam, S. N.; Suslick, K. S. *J. Am. Chem. Soc.* **1988**, *110*, 2011–2012. (c) Girolami, G. S.; Milam, S. N.; Suslick, K. S. *Inorg. Chem.* **1987**, *26*, 343–344. (d) Milam, S. N. Doctoral Thesis, University of Illinois at Urbana-Champaign, 1989.

(6) Yan, X.; Holten, D. *J. Phys. Chem.* **1988**, *92*, 409–414.

(7) (a) Donohoe, R. J.; Duchowski, J. K.; Bocian, D. F. *J. Am. Chem. Soc.* **1988**, *110*, 6119–6124. (b) Duchowski, J. K.; Bocian, D. F. Submitted for publication.

(9) Longuet-Higgins, H. C. *J. Chem. Phys.* **1950**, *18*, 265.

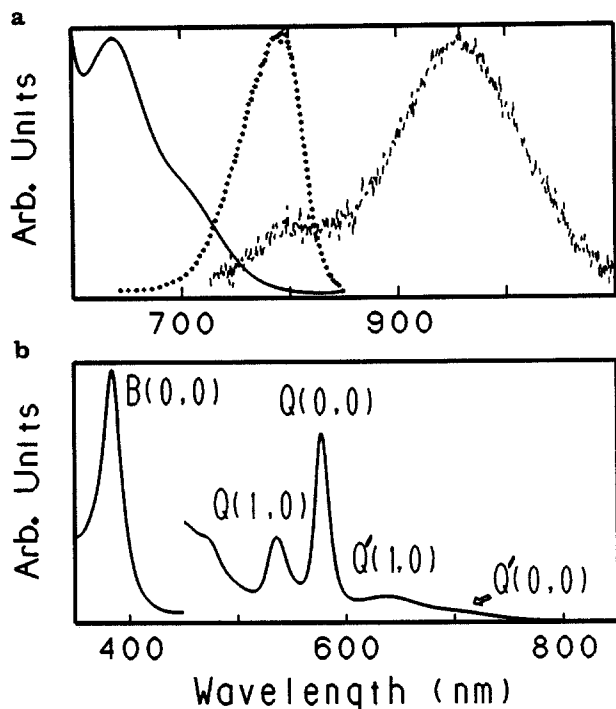


**Figure 1.** (a) Absorption (solid line), fluorescence (dotted line), and phosphorescence (dashed line) spectra of  $\text{Th}(\text{OEP})_2$  in toluene at 295 K. The weak emission near 790 nm in the dashed-line spectrum is primarily due to fluorescence. Excitation spectra verify that the emission features arise from the parent compound. (b) Absorption spectra of  $\text{Th}(\text{OEP})_2$  between 350 and 850 nm in toluene at 295 K. The Soret, or B(0,0), absorption band has been scaled down by a factor of 10.

In nondegassed solutions at 295 K,  $\text{Th}(\text{OEP})_2$  has a broad asymmetric fluorescence emission centered near 790 nm ( $\phi_f \sim 10^{-5}$ ) and a short-wavelength tail that extends to near 700 nm (dotted line, Figure 1a).<sup>8,9a</sup> Degassed solutions of  $\text{Th}(\text{OEP})_2$  reveal a phosphorescence emission at 960 nm, in addition to fluorescence near 790 nm (dashed line, Figure 1a). Time-resolved absorption experiments on  $\text{Th}(\text{OEP})_2$  (and also on  $\text{Th}(\text{TPP})_2$ ) reveal an initial transient with a  $\sim 10$ -ps lifetime (probably the new, weakly fluorescing  $^1(\pi, \pi^*)$  state), which decays in high yield (>85%) into a relatively long-lived ( $\tau \sim 50 \mu\text{s}$ ) phosphorescent  $^3(\pi, \pi^*)$  state.<sup>9b</sup> This behavior contrasts with that of the analogous lanthanide porphyrin complexes,  $\text{Ce}(\text{OEP})_2$  and  $\text{Ce}(\text{TPP})_2$ , which are nonluminescent and deactivate in  $\sim 2$  ps after excitation.<sup>10</sup>

The fluorescence spectrum of  $\text{Th}(\text{OEP})_2$  bears a mirror-symmetry relationship to the weak ground state absorption band near 710 nm and the stronger band  $\sim 1500 \text{ cm}^{-1}$  to the blue, near 640 nm (solid line, Figure 1). The  $\sim 1500\text{-cm}^{-1}$  spacing is similar to the vibrational spacing typically seen in the absorption and emission spectra of porphyrins,<sup>11,12</sup> including the spacing between

the Q(0,0) and Q(1,0) bands in the spectra of the  $\text{Th}^{\text{IV}}$  sandwich complexes (Figure 1b). The strong similarity between the ground state absorption spectra of the  $\text{Th}^{\text{IV}}$ ,  $\text{Ce}^{\text{IV}}$ , and  $\text{U}^{\text{IV}}$  sandwich complexes<sup>3-5</sup> suggests that the origin of the lowest energy  $^1(\pi, \pi^*)$  excited state in all of these complexes, which we call the  $^1Q'(\pi, \pi^*)$  state, is located in the vicinity of 700 nm. The very small amplitude of the (0,0) transition suggests that it is essentially dipole forbidden. We therefore attribute the stronger absorption near 640 nm to the  $^1Q'(1,0)$  vibronic transition and the fluorescence band at  $\sim 790$  nm to the  $^1Q'(0,1)$  vibronic transition. Both transitions may derive their strength from vibronic coupling with the higher energy Soret (B) state (and possibly also with  $^1Q'(\pi, \pi^*)$ ), as is typical in porphyrin spectra.<sup>11</sup>

A broad absorption between 600 and 700 nm is characteristic of closely spaced porphyrin dimers. It is seen not only in porphyrin sandwich complexes but also in cofacial  $\text{Ru}^{\text{II}}$  porphyrin dimers that contain a direct metal-metal double bond.<sup>13</sup> In all of these complexes, the core atoms of the two macrocycles are held within  $\sim 3.5 \text{ \AA}$ , and the central nitrogen atoms of the rings are even closer ( $\sim 2.8 \text{ \AA}$ ).<sup>3,5,13</sup> The new red-region absorption bands are absent in the spectra of porphyrin monomers<sup>11</sup> and cofacial porphyrin dimers with larger spacings between the rings, such as those bridged by single atoms (e.g.,  $\mu$ -oxo complexes) and those containing flexible linkages (e.g., face-to-face porphyrins).<sup>12,14</sup> Since excitonic interactions cannot explain the new  $^1Q'(\pi, \pi^*)$  manifold  $\sim 3000 \text{ cm}^{-1}$  below the normal  $^1Q(\pi, \pi^*)$  manifold,<sup>15</sup> we conclude that the new  $^1Q'(\pi, \pi^*)$  state is a manifestation of the strong orbital overlap that must be present whenever porphyrins are brought within  $\sim 3 \text{ \AA}$  of one another.

In a simple one-electron MO picture, the dimer HOMO is the antibonding (i.e., antisymmetric) combination of the HOMOs of the two monomers, and the dimer LUMO is the bonding (i.e., symmetric) combination of the monomer LUMOs.<sup>7</sup> The observation of new  $(\pi, \pi^*)$  absorption, fluorescence, and phosphorescence bands that are  $\sim 3000 \text{ cm}^{-1}$  lower in energy than those of the corresponding monomers suggests that the interaction energies between the relevant orbitals of the two monomeric subunits are of the order of  $10^3 \text{ cm}^{-1}$ . In fact, such strong orbital interactions provide an explanation<sup>7</sup> for the appearance of a near-IR band in the ground state absorption spectrum of the oxidized sandwich complexes.<sup>3,5,7</sup> Strong orbital interactions have also been postulated in recent theoretical studies of other closely spaced cofacial porphyrins<sup>16</sup> and of the dimeric primary electron donor in the photosynthetic reaction center.<sup>17</sup> It is difficult at present, however, to pinpoint the orbital parentage of the new low-energy  $^1Q'(\pi, \pi^*)$  state, since configuration interaction is likely to be significant.<sup>16,17</sup>

(11) Gouterman, M. In *The Porphyrins*; Dolphin, D., Ed.; Academic Press: New York, 1979; Vol. III, pp 1-165.

(12) Gouterman, M.; Holten, D.; Lieberman, E. *Chem. Phys.* **1977**, *25*, 139-153. (b) Chang, C. K. *J. Heterocycl. Chem.* **1977**, *14*, 1285-1288. (c) Collman, J. P.; Barnes, C. E.; Collins, T. J.; Brothers, P. J. *J. Am. Chem. Soc.* **1981**, *103*, 7030-7033. (d) Leighton, P.; Cowan, J. A.; Abraham, R. J.; Sanders, J. K. M. *J. Org. Chem.* **1988**, *53*, 733-740. (e) Osuka, A.; Maruyama, K. *J. Am. Chem. Soc.* **1988**, *110*, 4454-4456. (f) Shelnutt, J. A.; Dobry, M. M.; Saterlee, J. D. *J. Chem. Phys.* **1984**, *88*, 4980-4987.

(13) (a) Collman, J. P.; Prodollier, J. W.; Leidner, C. R. *J. Am. Chem. Soc.* **1986**, *108*, 2916-2912. (b) Collman, J. P.; Barnes, C. E.; Swepston, P. N.; Ibers, J. A. *J. Am. Chem. Soc.* **1984**, *106*, 3500-3510.

(14) Some single atom-bridged iron porphyrin dimers have absorptions to the red of 600 nm, but these may be due to d-d or charge-transfer transitions that are also present in iron porphyrin monomers (see: Bocian, D. F.; Findsen, E. W.; Hoffman, J. A., Jr.; Schick, G. A.; English, D. R.; Hendrickson, D. N.; Suslick, K. S. *Inorg. Chem.* **1984**, *23*, 800-807).

(15) As in weakly coupled porphyrin dimers,<sup>12,14</sup> exciton coupling of the strong Soret transitions of the monomers can explain the blue shift of the Soret band (and possibly also the appearance of a weak feature near 480 nm) in the sandwich complexes (see Figure 1b). This mechanism cannot, however, explain the presence of the  $^1Q'(\pi, \pi^*)$  state below the  $^1Q(\pi, \pi^*)$  state, since exciton coupling of the weak monomer  $Q(\pi, \pi^*)$  transitions should be negligible. Similarly, exciton coupling cannot explain the Q bands of  $\text{Ce}(\text{OEP})(\text{TTP})$  if these do not resemble the Q bands of lanthanide OEP and TPP monomers, whereas the Q bands of  $\text{Ce}(\text{OEP})_2$  and  $\text{Ce}(\text{TPP})_2$  are very similar to the Q bands of the corresponding monomers.<sup>4</sup>

(16) Petke, J. D.; Maggiora, G. M. *J. Chem. Phys.* **1986**, *84*, 1640-1652.

(17) (a) Thompson, M. A.; Zerner, M. C. *J. Am. Chem. Soc.* **1988**, *110*, 606-607. (b) Scherrer, P. O. J.; Fischer, S. F. *Chem. Phys.* **1989**, *131*, 115-127.

(8) Abbreviations: OEP is 2,3,7,8,12,13,17,18-octaethylporphinate(2-); TPP is 5,10,15,20-tetraphenylporphinate(2-).

(9) (a) Luminescence spectra were measured on a Spex spectrofluorometer with 5-nm excitation and detection bandwidths. The apparatus was equipped with either a Hamamatsu R928 photomultiplier tube and a photon counter (dotted line, Figure 1a) or an RCA C30956E silicon avalanche photodiode and lock-in detection (dashed line, Figure 1a). Absorption spectra were measured on a Perkin-Elmer Lambda 3B spectrophotometer. (b) For fast transient absorption measurements, the samples were excited with a 582-nm, 150- $\mu\text{J}$ , 350-fs pulse and probed with a broad-band pulse at delay times up to several nanoseconds. The  $^3(\pi, \pi^*)$  lifetime was measured via ground state absorption recovery with an apparatus utilizing 532-nm, 10-mJ, 10-ns pulses. Details of the time-resolved absorption studies will be reported elsewhere.

(10) (a) The  $\text{Ce}^{\text{IV}}$  sandwich complexes are nonemissive<sup>3d,4,6</sup> and deactivate, in  $\sim 2$  ps after excitation, to the ground electronic state via a ring-to-metal charge-transfer excited state.<sup>4</sup> On the basis of redox potentials, it is expected that such an excited state lies at low energy in the  $\text{Ce}^{\text{IV}}$  complexes,<sup>1a,7a</sup> but above the  $^1Q(\pi, \pi^*)$  state in the  $\text{Th}^{\text{IV}}$  complexes.<sup>3</sup> (b) The lack of fluorescence from a  $\text{Sn}^{\text{IV}}$  phthalocyanine sandwich complex has been attributed to quenching by a low-energy charge-resonance state not seen in the electronic spectrum (Ohno, O.; Ishikawa, N.; Matsuzawa, T.; Kobayashi, H. *J. Phys. Chem.* **1989**, *93*, 1713-1718).

as it is between the four-orbital configurations in the monomer.<sup>11</sup> From an alternative viewpoint, the new low-energy  $^1Q'(\pi, \pi^*)$  excited state results from the coupled exciton and charge-resonance states of the dimer.<sup>18</sup> The extent of mixing among these states is of central importance in understanding the properties of the bacteriochlorophyll dimer in the photosynthetic reaction center.<sup>1c,d,17b,19</sup>

The spectroscopic results presented here for the  $\text{Th}^{\text{IV}}$  sandwich complexes have identified a new low-energy  $(\pi, \pi^*)$  state that apparently arises from the significant overlap that should be present whenever porphyrin rings are held within  $\sim 3 \text{ \AA}$  of one another. The weak origin and stronger overtone transitions to this lowest  $^1(\pi, \pi^*)$  excited state account for the absorption bands in the 600–700-nm region in strongly interacting porphyrin dimers. The relative intensities of these transitions suggest that vibronic coupling is important in these dimers, as has been proposed for the bacteriochlorophyll special pair of the photosynthetic reaction center.<sup>1d,19b</sup> Our observations on these simple, well-defined sandwich complexes should aid in evaluating the nature of the lowest excited state of the special pair, where exciton and protein effects may also contribute.

**Acknowledgment.** This work was supported in part by Grants GM34685 and HL25934 from the National Institutes of Health. Receipt of an NIH Career Development Award (K.S.S.), a Sloan Foundation Research Fellowship (G.S.G. and K.S.S.), and a Dreyfus Foundation Teacher-Scholar Award (G.S.G.) are gratefully acknowledged. We thank L. McDowell for assistance with the phosphorescence measurements and Drs. D. Bocian, C. Kirmaier, R. Friesner, and M. Gouterman for helpful discussions.

(18) The exciton states are linear combinations of the local-excited configurations and the charge-resonance states are linear combinations of the charge-transfer, or ionic, configurations. Charge-resonance states have been discussed recently for the related  $\text{Sn}^{\text{IV}}$  phthalocyanine sandwich complex.<sup>10b</sup>

(19) (a) Parson, W. W.; Warshel, A. *J. Am. Chem. Soc.* **1987**, *109*, 6152–6163. (b) Won, Y.; Friesner, R. A. *J. Phys. Chem.* **1988**, *92*, 2214–2219.

## Enzyme-Mediated Asymmetric Decarboxylation of Disubstituted Malonic Acids

Kenji Miyamoto and Hiromichi Ohta\*

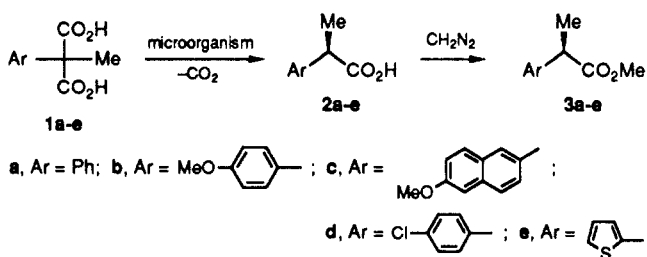
Department of Chemistry, Keio University  
Hiyoshi 3-14-1, Yokohama 223, Japan

Received December 5, 1989

Transformation of a prochiral molecule to a chiral product is one of the most attractive methods of asymmetric synthesis.<sup>1</sup> Although some efforts have been devoted to enantioselective decarboxylation of disubstituted malonates, only unsatisfactory results have been obtained so far.<sup>2</sup> Thus, we tried enzymatic conversion of the acids, because some biosynthetic routes, such as fatty acid synthesis, involve decarboxylation steps.

First, we screened for a microorganism that is able to grow by utilizing phenylmalonic acid as a sole source of carbon. It was supposed that the first step of the metabolism is decarboxylation giving phenylacetic acid, which would be further oxidized via benzoylformate. If the enzyme responsible for this reaction also acts on disubstituted malonic acids, then chiral acids are expected to be obtained because further metabolism to  $\alpha$ -keto acids is

Table I. Enzyme-Mediated Asymmetric Decarboxylation



entry	substrate	substrate concn, %	yield of <b>3</b> , %	ee, % (confign)	$[\alpha]_D$ , deg
1	<b>1a</b>	0.3	87	91 ( <i>R</i> )	
2	<b>1a</b>	0.4	93	96 ( <i>R</i> )	
3	<b>1a</b>	0.5	90	98 ( <i>R</i> )	-96 (c 1.1, EtOH) <sup>a</sup>
4	<b>1b</b>	0.1	48	99 ( <i>R</i> )	-71 (c 1.1, $\text{CHCl}_3$ ) <sup>b</sup>
5	<b>1b</b>	0.2	35	97 ( <i>R</i> )	
6	<b>1c</b>	0.3	95	>95 ( <i>R</i> )	
7	<b>1c</b>	0.5	96	>95 ( <i>R</i> )	-76 (c 1.0, $\text{CHCl}_3$ ) <sup>c</sup>
8	<b>1d</b>	0.3	95	98 ( <i>R</i> )	-67 (c 1.1, $\text{CHCl}_3$ )
9	<b>1d</b>	0.5	85	97 ( <i>R</i> )	
10	<b>1e</b>	0.3	98	95 ( <i>S</i> )	-40 (c 1.1, $\text{CHCl}_3$ )
11	<b>1e</b>	0.5	97	91 ( <i>S</i> )	

<sup>a</sup>Literature,<sup>4</sup> *S* form,  $[\alpha]_D^{25} +93.3^\circ$  (c 0.96, EtOH). <sup>b</sup>Literature,<sup>4</sup> *S* form,  $[\alpha]_D^{21} +75.3^\circ$  (c 1.02,  $\text{CHCl}_3$ ). <sup>c</sup>Literature,<sup>4</sup> *S* form,  $[\alpha]_D^{21} +78.4^\circ$  (c 1.05,  $\text{CHCl}_3$ ).

impossible. A number of soil samples were examined, and it was found that a few microorganisms grew on phenylmalonic acid. We then selected a bacterium identified as *Alcaligenes bronchisepticus*, which has the ability to realize the asymmetric decarboxylation of  $\alpha$ -methyl- $\alpha$ -phenylmalonic acid (**1a**). Fifty milliliters of an inorganic medium<sup>3</sup> containing peptone (50 mg) and phenylmalonic acid (250 mg) was inoculated with *A. bronchisepticus* and shaken for 4 days at 30 °C. To the resulting suspension was added 250 mg of **1a**, and the incubation was continued for an additional 5 days. The broth was extracted, esterified with diazomethane, and purified by preparative TLC, to afford optically active methyl  $\alpha$ -phenylpropionate (**3a**). The present enzyme system was applied to some analogous compounds, as summarized in Table I. When the aryl group was phenyl (**1a**), 2-(6-methoxynaphthyl) (**1c**), *p*-chlorophenyl (**1d**), and 2-thienyl (**1e**), the substrates afforded optically active  $\alpha$ -arylpropionic acid (**2a,c-e**) in high yields. On the other hand, in the case of *p*-methoxyphenyl-substituted malonate (**1b**), the yield of the desired product (**3b**) was low. The substrate specificity of this reaction is supposed to depend not only on the bulkiness of the aryl group but also on electronic factors.

The absolute configurations of **3a-c** were revealed to be *R* by comparison of the specific rotation with reported values.<sup>4</sup> Chloro derivative **3d** was reduced with  $\text{PdCl}_2\text{-NaBH}_4$  (90%), to give **3a**,<sup>5</sup> which exhibited  $[\alpha]_D -96^\circ$  (c 0.82, ethanol), indicating the absolute configuration to be *R*. Desulfurization (Raney Ni)<sup>6</sup> of **3e** followed by hydrolysis and hydrogenation afforded (*R*)-(-)- $\alpha$ -methylcaproic acid (total 44%),  $[\alpha]_D -16^\circ$  (c 3.8, ether). Thus the absolute configuration of **3e** is determined to be *S*.<sup>7</sup> Optical purities of the products (**3**) were determined by HPLC analysis (CHIRALCEL OJ) or 400-MHz  $^1\text{H}$  NMR measurements in the presence of a chiral shift reagent  $[\text{Eu}(\text{hfc})_3]$  (for **3c**).

In order to clarify the mechanism and examine the substrate specificities, the racemic monoethyl ester of **1a** was subjected to

(3) The inorganic medium consists of  $(\text{NH}_4)_2\text{HPO}_4$  (10 g),  $\text{K}_2\text{HPO}_4$  (2 g),  $\text{MgSO}_4 \cdot 7\text{H}_2\text{O}$  (300 mg),  $\text{FeSO}_4 \cdot 7\text{H}_2\text{O}$  (10 mg),  $\text{ZnSO}_4 \cdot 7\text{H}_2\text{O}$  (8 mg),  $\text{MnSO}_4 \cdot 4\text{H}_2\text{O}$  (8 mg), yeast extract (200 mg), and D-biotin (0.02 mg) in  $\text{H}_2\text{O}$  (1000 mL), pH 7.2.

(4) Honda, Y.; Ori, A.; Tsuchihashi, G. *Bull. Chem. Soc. Jpn.* **1987**, *60*, 1027–1036.

(5) Satoh, T.; Mitsuo, N.; Nishiki, M.; Nanba, K.; Suzuki, S. *Chem. Lett.* **1981**, 1029–1030.

(6) Badger, G. M.; Rodda, H. J.; Sasse, W. H. F. *J. Chem. Soc.* **1954**, 4162–4168.

(7) Terashima, S.; Tseng, C. C.; Koga, K. *Chem. Pharm. Bull.* **1979**, *27*, 747–757.

(1) (a) Schneider, M.; Engle, N.; Boensmann, H. *Angew. Chem., Int. Ed. Engl.* **1984**, *23*, 66–68. (b) Björkling, F.; Boutelje, J.; Gatenbeck, S.; Hult, K.; Norin, T. *Tetrahedron Lett.* **1985**, *26*, 4957–4958. (c) Kitazume, T.; Sato, T.; Kobayashi, T.; Lin, J. T. *J. Org. Chem.* **1986**, *51*, 1003–1006. (d) Björkling, F.; Boutelje, J.; Gatenbeck, S.; Hult, K.; Norin, T.; Szmlik, P. *Tetrahedron* **1985**, *41*, 1347–1352. (e) Scheffold, R., Ed. *Modern Synthetic Methods*; Springer-Verlag: Berlin, Heidelberg, 1989.

(2) (a) Toussaint, O.; Capdevielle, P.; Maumy, M. *Tetrahedron Lett.* **1987**, *28*, 539–542. (b) Verbit, L.; Halbert, T. R.; Patterdon, R. B. *J. Org. Chem.* **1975**, *40*, 1649–1650.